Meteoritics, 200–213 (1994)

Watson: A new link in the IIE iron chain

EDWARD OLSEN[1], ANDREW DAVIS[2], ROY S. CLARKE, JR.[3], LUDOLF SCHULTZ[4], HARTWIG W. WEBER[4], ROBERT CLAYTON[1,2,5], TOSHIKO MAYEDA[2], EUGENE JAROSEWICH[3], PAUL SYLVESTER[1,8], LAWRENCE GROSSMAN[1], MING-SHENG WANG[6], MICHAEL E. LIPSCHUTZ[6], IAN M. STEELE[1] AND JAMES SCHWADE[7]

[1]Dept. of the Geophysical Sciences, University of Chicago, Chicago, Illinois 60637, USA
[2]Enrico Fermi Institute, University of Chicago, Chicago, Illinois 60637, USA
[3]Dept. of Mineral Sciences, National Museum of Natural History, Smithsonian Institution, Washington, D.C. 20560, USA
[4]Max-Planck Institut für Chemie, D-55020 Mainz, Germany
[5]Dept. of Chemistry, University of Chicago, Chicago, Illinois 60637, USA
[6]Dept. of Chemistry, Purdue University, West Lafayette, Indiana 47907, USA
[7]Olivet Nazarene University, Kankakee, Illinois 60901, USA
[8]Current address: Australian National University, Canberra, ACT 2611, Australia

(Received 1993 June 18; accepted in revised form 1993 November 21)

Abstract—Watson, which was found in 1972 in South Australia, contains the largest single silicate rock mass seen in any known iron meteorite. A comprehensive study has been completed on this unusual meteorite: petrography, metallography, analyses of the silicate inclusion (whole rock chemical analysis, INAA, RNAA, noble gases, and oxygen isotope analysis) and mineral compositions (by electron microprobe and ion microprobe). The whole rock has a composition of an H-chondrite minus the normal H-group metal and troilite content. The oxygen isotope composition is that of the silicates in the IIE iron meteorites and lies along an oxygen isotope fractionation line with the H-group chondrites. Trace elements in the metal confirm Watson is a new IIE iron. Whole rock Watson silicate shows an enrichment in K and P (each ≈2X H-chondrites). The silicate inclusion has a highly equilibrated igneous (peridotite-like) texture with olivine largely poikilitic within low-Ca pyroxene: olivine (Fa_{20}), opx ($Fs_{17}Wo_3$), capx (Fs_9Wo_{41}) (with very fine exsolution lamellae), antiperthite feldspar ($An_{1-3}Or_5$) with <1 μm exsolution lamellae ($An_{1-3}Or_{>40}$), shocked feldspar with altered stoichiometry, minor whitlockite (also a poorly characterized interstitial phosphate-rich phase) and chromite, and only traces of metal and troilite. The individual silicate minerals have normal chondritic REE patterns, but whitlockite has a remarkable REE pattern. It is very enriched in light REE (La is 720X C1, and Lu is 90X C1, as opposed to usual chonditic values of ≈300X and 100–150X, respectively) with a negative Eu anomaly. The enrichment of whole rock K is expressed both in an unusually high mean modal Or content of the feldspar, Or_{13}, and in the presence of antiperthite.

Whole rock trace element data for the silicate mass support the petrography. Watson silicate was an H-chondrite engulfed by metal and melted at >1550 °C. A flat refractory lithophile and flat REE pattern (at ≈1x average H-chondrites) indicate that melting took place in a relatively closed system. Immiscible metal and sulfide were occluded into the surrounding metal host. Below 1100 °C, the average cooling rate is estimated to have been ≈1000 °C/Ma; Widmanstätten structure formed, any igneous zoning in the silicates was equilibrated, and feldspar and pyroxene exsolution took place. Cooling to below 300 °C was completed by 3.5 Ga B. P. At 8 Ma, a shock event took place causing some severe metal deformation and forming local melt pockets of schreibersite/metal. This event likely caused the release of Watson into interplanetary space. The time of this event, 8Ma, corresponds to the peak frequency of exposure ages of the H-chondrites. This further confirms the link between IIE irons and the H-chondrites, a relationship already indicated by their common oxygen isotope source.

Watson metal structures are very similar to those in Kodaikanal. Watson, Kodaikanal and Netschaëvo form the young group of IIE meteorites (ages 3.7 ± 0.2 Ga). They appear to represent steps in a chain of events that must have taken place repeatedly on the IIE parent body or bodies from which they came: chondrite engulfed in metal (Netschaëvo); chondrite melted within metal (Watson); and finally melted silicate undergoing strong fractionation with the fractionated material emplaced as globules within metal (Kodaikanal). Watson fills an important gap in understanding the sequence of events that took place in the evolution of the IIE-H parent body(ies). This association of H-chondrite with IIE metal suggests a surface, or near surface process—a suggestion made by several other researchers.

INTRODUCTION

The Watson iron meteorite (93 kg) was found in 1972 near Watson, South Australia (30°29'S, 131°30'E). It was first cut in 1990. The second slice (19 x 24 cm) revealed a large mass of silicate rock embedded in the metal (Fig. 1), an estimated 30 cm^3 and 110 g in the slab. The total size of the mass is substantially larger. This is a part of the largest single silicate mass known within an iron meteorite. Two polished thin sections were made from silicate chips taken from positions 6 cm apart on the reverse side of the mass that is shown in Fig. 1.

Examination of these sections lead us to suspect, as we demonstrate below, that Watson silicate was originally a mass of H-chondrite that was engulfed in metal, melted, and then recrystallized. Watson, therefore, provides an opportunity to examine the concurrent thermal histories recorded by a melted chondrite mass and its enclosing metal host. The following study shows that Watson is a IIE iron with silicate inclusions and has physical properties intermediate between those of two other IIE irons with silicate inclusions, Netschaëvo and Kodaikanal.

EXPERIMENTAL METHODS AND RESULTS

Petrography of the Silicate Mass

Optical and SEM examination showed that both sections are identical in their petrographic features. Examination of the entire surface of the silicate mass with a binocular microscope does not reveal any significant inhomogeneities such as veins, large scale mineralogical segregations, or an obvious overall fabric.

The rock has an igneous texture like that of terrestrial peridotite. Orthopyroxene crystals, 400 to 1000 μm, contain numerous poikilitically enclosed crystals of subhedral to euhedral olivine. The olivine crystals range from 10 μm to 100 μm; the mode is 50–60 μm. Some subhedral and euhedral olivine crystals are also interstitial to orthopyroxene. Calcic

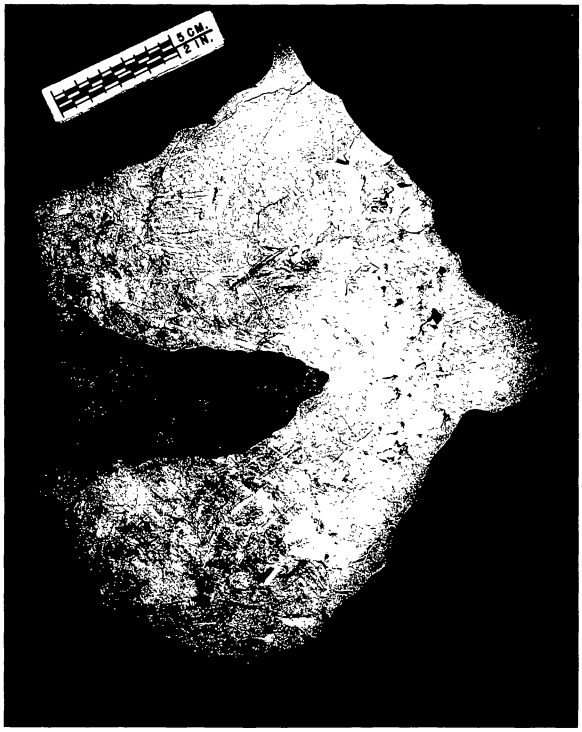

FIG. 1. Polished surface of second slice from the original Watson mass showing the large silicate inclusion. Both distorted and relatively undistorted Widmanstätten structure can be seen.

pyroxene occurs as interstitial, irregular, anhedral grains, 200 to 400 μm in greatest dimension. Troilite and feldspar are interstitial and irregular in shape. Feldspar occurs in two physical forms: (1) highly fractured, sheared-looking, optically cloudy material that occurs between pyroxene and olivine grains; and (2) masses of feldspar that are optically clearer and are also interstitial to pyroxene and olivine. Some of the clearer-looking feldspars also occur as small angular grains within and bordering the cloudy feldspar masses. Widely separated chromite grains, 200 to 350 μm, range from euhedral to anhedral. Metal occurs sparsely as rounded grains <5 to 20 μm, most often in composite grains with troilite. Whitlockite occurs sparsely as irregular grains (30 to 100 μm) between orthopyroxene, olivine, and calcic pyroxene. Careful X-ray scanning for P revealed the presence of thin meandering stringers, up to several tens of μm in length, of a P-bearing phase or phases between some of the silicate grain boundaries. This material could not be analyzed because it is never more than 2 μm wide. Its energy-dispersive X-ray spectrum shows that it contains major P with variable amounts of Ca, Mg, Al, Si, S, and Fe. Two spectra showed small amounts of K, Cr, and Cl. The Si, Al, Mg and some of the Fe is certainly due to beam overlap onto adjacent silicate phases. Modal weight percentages were calculated from the bulk analysis (Table 1) and mineral analyses (Table 2): 57% olivine, 23% orthopyroxene, 5% calcium pyroxene, 12% feldspar, 0.4% chromite, 0.9% troilite, 1% phosphate phases (whitlockite plus the uncharacterized phosphate alteration material), and 0.3% metal. Ilmenite, a phase known in H chondrites and some IIE irons, was not found.

Watson does not have any of the textural features of silicates found in other IIE irons, such as chondrules in Netschaëvo and pyroxene-feldspar corona structures in Elga, Kodaikanal, and Weekeroo Station (Bunch *et al.*, 1970; Osadchii *et al.*, 1981). Watson, Netschaëvo, Elga and Kodaikanal contain olivine, whereas Colomera and Weekeroo Station do not.

Mineral Compositions of Silicates

Wavelength-dispersive electron microprobe analyses were made using a Cameca SX-50 operated at 15 kV with a beam current of 25 nA. The beam was sometimes defocused and counting times were minimized to avoid alkali loss in analyses of feldspars. Compositions of the major minerals are given in Table 2. Olivine ($Fa_{20.60 \pm 0.23}$), orthopyroxene ($Fs_{17.56 \pm 0.19}Wo_{3.75 \pm 0.34}$), and calcic pyroxene ($Fs_{9.00 \pm 0.32}Wo_{40.95 \pm 0.49}$) grains have fairly uniform unzoned compositions from grain to grain and within grains (all $\pm$ values are 1 σ). The H-chondrites contain Fa_{16-20} olivine (Dodd, 1981); the IIE irons Elga, Kodaikanal, and Netschaëvo contain Fa_{22}, Fa_{21}, and Fa_{14}, respectively (Bunch *et al.*, 1970; Osadchii *et al.*, 1981). Pyroxene compositions in H-chondrites are Fs_{14-18}. Pyroxene compositions in IIE irons are as follows: Colomera ($Fs_{23}Wo_2$, $Fs_{9-14}Wo_{40-46}$), Elga ($Fs_{15-16}Wo_{0.4-3}$, $Fs_{9-12}Wo_{41-44}$), Kodaikanal ($Fs_{17}Wo_3$, $Fs_{8-10}Wo_{37-43}$), Netschaëvo ($Fs_{14}Wo_1$, Fs_6Wo_{45}), and Weekeroo Station ($Fs_{22}Wo_3$, $Fs_{18}Wo_{36}$) (Bunch *et al.*, 1970; Osadchii *et al.*, 1981). The calcic pyroxenes in Watson contain very closely spaced sub μm lamellae which are unavoidable and too narrow to analyze.

Microprobe analyses of the cloudy feldspar masses give poor totals and stoichiometries; analyses, normalized to 8 O, show alkali deficiencies. The ranges of cloudy feldspar compositions are $An_{3.0-4.3}Or_{5.7-6.7}$. The clearer feldspar grains give analyses with good stoichiometries, with ranges of $An_{1.4-3.0}$ and Or_{5-40}. Under careful examination, the apparent large variation in orthoclase content in the clear feldspar is due to exsolution of K feldspar from the albitic host (*i.e.,* antiperthite). Backscattered electron images reveal K-rich lamellae of about 0.3 μm width, spaced 1 to 3 μm apart. The narrow width of the lamellae made it impossible to avoid beam overlap onto adjacent albitic feldspar during electron microprobe analyses. The best possible analysis of such a K-rich lamella is given in Table 2 with an analysis of its coexisting albitic host: $An_{1.43}Or_{41.42}$, $An_{2.18}Or_{5.17}$, respectively. This Watson feldspar is similar in An and Or content to that in Kodaikanal ($An_{1-3}Or_{4-44}$) and lower in An and Or content than that in Weekeroo Station ($An_{9-11}Or_{5-27}$) and Netschaëvo ($An_{14}Or_4$) (Bunch and Olsen, 1968; Bunch *et al.*, 1970). Because of the two physical conditions of the feldspar (*i.e.,* the variability in composition of the cloudy material and the exsolution lamellae within the better preserved feldspar grains), it is not possible to obtain an accurate idea of the average feldspar composition of the whole rock in order to compare it with the average composition of feldspar found in H chondrites, $An_{12}Or_6$ (Dodd, 1981). In calculating the mode, however, (allowing for the Ca and Na contents of pyroxenes and whitlockite) a value of approximately $An_{10}Or_{13}$ is derived. This bulk An content is close to that of average H-chondrites, but the Or content is high by about 2x the average. As we note later (*cf.* Bulk Wet Chemical Analysis of the Silicate below), total K is enriched by about 2x above average H-chondrites.

Metal within the silicate mass has wide variations in Ni content within single grains. One bead, for example, has Ni concentrations ranging from 7% to 22%. It is possible the variations are due to an unresolvable fine-scale Widmanstätten structure.

Table 1. Bulk Chemical Analysis of the Silicate Inclusion in the Watson Meteorite (E. Jarosewich, Analyst)

	A	B	C	D
SiO_2	45.51	35.22	36.60	-----
TiO_2	0.14	0.11	0.12	-----
Al_2O_3	2.54	1.97	2.14	-----
Cr_2O_3	0.49	0.38	0.52	-----
FeO	13.18	10.20	10.30	-----
MnO	0.37	0.29	0.31	-----
MgO	31.41	24.31	23.26	-----
CaO	2.29	1.77	1.74	-----
Na_2O	1.08	0.84	0.86	-----
K_2O	0.28	0.22	0.09	-----
P_2O_5	0.60	0.46	0.27	-----
H_2O+	0.14	0.11	0.32	-----
H_2O-	0.04	0.03	0.12	-----
Fe(metal)	0.24	15.98	15.98	90.97*
Ni	0.13	1.74	1.74	8.21
Co	<0.01	0.08	0.08	0.44
FeS	0.85	5.43	5.43	-----
C	ND	0.00	0.11	-----
P				0.38
Total	99.29	99.14	99.99	100.00
Total Fe	11.02	27.36	27.45	-----

A Original analysis of silicate sample
B Fe(metal), FeS, Ni, and Co added for average H-chondrite
C Average composition of H-chondrites (Jarosewich, 1990)
D Bulk composition of metal
ND = not determined. * Fe by difference.

Table 2. Representative Microprobe Analyses of Minerals in Watson

	Olivine	Opx	Capx	Feld*	Feld**	Chrom	Whit
Na_2O	0.00	0.09	0.84	10.11	6.20	0.00	2.18
MgO	40.40	28.64	16.39	0.00	0.00	5.66	3.69
Al_2O_3	0.01	0.51	0.74	19.04	18.29	6.94	0.02
SiO_2	39.32	56.39	54.15	67.06	67.05	0.04	0.15
P_2O_5	0.02	0.00	0.02	0.00	0.00	0.00	45.93
K_2O	0.00	0.00	0.00	0.84	6.83	0.00	0.05
CaO	0.04	1.88	19.06	0.43	0.28	0.02	47.56
TiO_2	0.02	0.16	0.34	0.00	0.00	2.20	0.02
Cr_2O_3	0.06	0.71	1.57	0.00	0.00	58.48	0.00
MnO	0.45	0.46	0.30	0.00	0.00	1.51	0.03
FeO	18.71	11.23	5.58	0.61	0.29	25.64	0.86
NiO	0.00	0.00	0.03	0.00	0.00	0.00	0.03
	99.03	100.07	99.02	98.09	98.94	100.49	100.52
Fa%	20.63	—	—	—	—	—	—
Fs%	—	17.36	9.42	—	—	—	—
Wo%	—	3.72	41.24	—	—	—	—
An%	—	—	—	2.18	1.43	—	—
Or%	—	—	—	5.07	41.42	—	—

* Low K albite host.
** High K lamella (*cf.* text)

Trace quantities of the same silicate phases described above are also found as isolated blebs along kamacite-kamacite grain boundaries outside the silicate mass within the host metal. These silicates consist of small amounts of olivine, low-Ca and high-Ca pyroxenes, and feldspar in isolation or together in various proportions. The compositions of both pyroxenes are similar to the pyroxenes within the large silicate mass: low-Ca pyroxenes average $Fs_{17.9}Wo_{3-4}$. Calcic pyroxene is rare, occurring interstitially as small patches between low-Ca pyroxenes. Only one good analysis could be obtained of one grain of it: $Fs_{9.7}Wo_{40.8}$. Although individual olivine grains are unzoned, there are grain to grain composition variations in the range $Fa_{18.8}$ to $Fa_{20.6}$. The latter value is the same composition as olivine in the nearby large silicate mass. As stated above, the silicates are present in only trace amounts in the metal, and the feldspar material is much less abundant in the metal than the other silicates. It is like the cloudy feldspar seen in the silicate mass and has poor stoichiometry. Feldspar compositions vary, for example, $An_{51.0}Or_{4.0}$, $An_{45.1}Or_{12.5}$, and $An_{53.7}Or_{4.3}$. These are considerably more calcic than feldspar within the main silicate mass; although because of the sparsity of feldspar in the metal, the sample size is too small to know if these compositions are typical or not.

Metallography of the Metal Host

Visual examination of a 220 cm^2 macro-etched metal surface reveals a hectic and confused structure containing areas of fine Widmanstätten pattern (WP) that have been locally distorted by a shock event (Fig. 1). Watson's primary WP developed in polycrystalline taenite (γ) with individual γ crystals, 1 to 3 cm across, resulting in numerous independent sites of WP initiation. Upon cooling the parent γ/γ grain boundaries transformed to kamacite/kamacite (α/α) boundaries. Distributed sporadically along these α/α boundaries are mm, to as long as a cm, inclusions consisting of schreibersite that may be associated with small amounts of silicates (described earlier). Troilite is much less abundant than schreibersite and tends to be associated preferentially with the silicates. The smaller ones of these inclusions tend to be rounded, while the larger ones are sinuous and elongated, with length to width ratios of 10 to 20. Some are dark colored and unidentifiable in macro sections. Several shear-zone structures with widths of less than one mm and lengths up to 10 cm traverse the section along former parent crystal (γ) grain boundaries; on occasion, they pass through metal crystals (*i.e.*, not along grain boundaries). At a macro level, Watson's metal bears strong structural and chemical similarities to the Kodaikanal IIE meteorite. While Kodaikanal is also very shocked, Watson appears to be more severely shocked. Watson does not possess the rounded silicate inclusions ("globules") dispersed throughout the metal so common in Kodaikanal. Structural relationships between Kodaikanal and other IIE meteorites, including Verkhne Dnieprovsk (see below), have been discussed by a number of authors (Axon, 1968; Bence and Burnett, 1969; Buchwald, 1975; Scott and Wasson, 1976; Bevan *et al.*, 1979; Prinz *et al.*, 1983; Wasson and Wang, 1986; Buchwald and Clarke, 1987; Armstrong *et al.*, 1990).

A microscope view of an area of relatively undisturbed WP from within a single parent crystal is shown in Fig. 2a. Kamacite bands consist of stubby α crystals, 100 to 200 μm, with varying length to width ratios. An estimated α band width is 0.08 mm;

occasionally broader α bands occur with schreibersite(s) at their centers. In the least distorted α areas, Neumann bands are abundant and straight; these become sinuous and finally fade completely where they project into a shocked area. Schreibersites are abundant (consistent with the rather high bulk P content), ranging up to 25 μm along α/α grain boundaries and to 50 x 200 μm within broader α bands. Occasional concentrations of larger schreibersites are observed in the centers of comparatively large α regions; these appear to be the sites of previously existing parent γ/γ grain boundaries. Taenite lamellae are mainly narrow, generally 2 to 5 μm but occasionally widening to over 15 μm. Plessite areas of several types occur. A few dark etching plessite fields with martensitic interiors are unevenly distributed and typically small (50 x 100 μm). The WP areas in Watson also show close similarity at a micro scale to typical structural areas in Kodaikanal (Fig. 2b).

A distinctive feature of Watson metal, one that has not been observed before as an important feature of a large volume of metal (93 kg), is the presence of numerous and pervasive dendritic melt pockets. These pockets are associated with the presence of schreibersite in regions of distortion along pre-existing parent crystal grain boundaries, and they may also be associated with silicates. The first reports of such structures were from the small surviving fragments of the Verkhne Dnieprovsk IIE meteorite in the London and Vienna collections (Bevan *et al.*, 1979; Buchwald and Clarke, 1987). A 2-mm Watson melt pocket with associated distortion structures is shown in Fig. 3. A 1.2-mm electron microprobe traverse (46 points of varying step lengths) was made for Ni, P, and S from its center to the middle of its lower left edge. Sulfur was below detection (<0.1 wt%) over the whole distance. Nickel values were rather consistent at 10.2 ± 0.1 wt% ; P values were more variable at 3.0 ± 0.8 wt%; a similar traverse over a smaller melt pocket gave Ni values of 10.9 ± 0.4 wt% and P values of 4.4 ± 0.5 wt% (1σ for all values). These values are similar to those reported earlier for melt pockets in Verkhne Dnieprovsk (Bevan *et al.*, 1979; Buchwald and Clarke, 1987). The metal structure to the left and the bottom of the melt pocket in Fig. 3 is curved into a mildly distorted form but is clearly a WP that has not been severely reheated. The light areas within the dark melt pocket are shock-heated, undissolved metal.

The area to the upper right in Fig. 3 is highly distorted WP. Figure 4 is an enlarged view of the base of the narrow neck of the melt pocket near the top of this structure in Fig. 3. The dark inverted funnel-shaped area on the left side of Fig. 4 has a very fine dendritic structure that is typical of the whole melt pocket. The kamacite on both sides of the neck has been heated and transformed to martensitic α_2 structure, indicating a temperature of over 700 °C for a brief period. Outside the α_2 area, where temperatures were lower, shock-hatched ϵ structure is present; this indicates shock levels above 130 kbar. Minus the compression and distortion, this structural association is typical

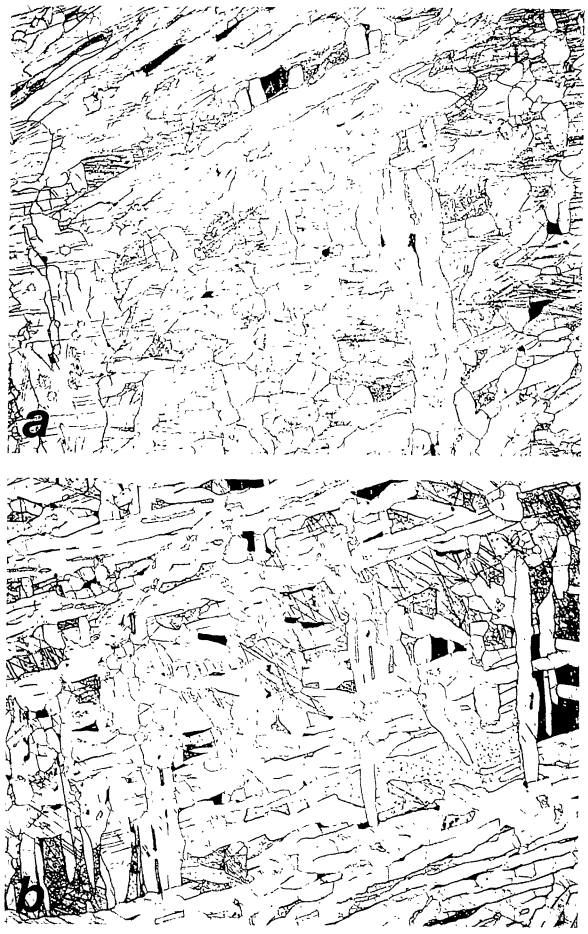

Fig. 2 (a) Relatively undisturbed Widmanstätten structure from within a single parent taenite crystal in Watson. Dark etching plessite with martensitic interiors is unevenly distributed. Area is 3.4 mm wide. (b) Very similar structures present in the IIE iron Kodaikanal (same scale).

FIG. 3. Mosaic showing dendritic melt pocket in Watson metal. Melted schreibersite pocket contains islands of unmelted kamacite remnants. Highly distorted Widmanstätten structure in the surrounding metal is in upper left quadrant of figure. Structure is mildly distorted to the left and below the melt pocket. The figure is 5 mm wide.

FIG. 4. Enlarged view of upper part of melt pocket illustrated in Fig. 3 showing fine dendritic structure typical of the melt pocket. Kamacite on both sides of the upper projection has been transformed to a martensitic α_2 structure. Field of view is 620 μm wide.

of heat-altered (Earth entry) ablation zones. This particular inclusion, however, is at least 1 cm below the nearest heat-altered meteorite surface zone, and it is surrounded by metal that has been unaltered. It is clearly an original, pre-terrestrial feature.

Oxygen Isotopic Composition of the Bulk Silicate

The oxygen isotope composition obtained on a bulk sample is $\delta^{17}O = +2.84, \delta 18O = +4.22‰$. This composition coincides with the mean H-chondrite composition (Clayton *et al.*, 1991) and the middle of the fractionation line passing through the silicate inclusions in the IIE iron meteorites (Clayton *et al.*, 1983). Based on this, we conclude that Watson is a new member of the IIE group.

Bulk Wet Chemical Analysis of the Silicate

A bulk sample of 3 g was analyzed by chemical methods combined with some instrumental methods (Jarosewich, 1990). The analysis (Table 1) cannot be compared directly to results for any chondrite meteorite group because the metal content is extremely low. It clearly differs from that of eucrites and howardites (Jarosewich, 1990). If, however, the average metal and troilite contents of an H-group chondrite are added to the analysis, the renormalized Watson bulk silicate matches an H-group chondrite very well (Col.B, Table 1). The only exceptions are K_2O and P_2O_5, each enriched by ≈2x over average H-group values.

Bulk Trace Element Analyses by INAA and RNAA

A fragment of bulk Watson silicate weighing approximately 500 mg was thoroughly powdered and mixed; an aliquot of 0.3 mg was taken for instrumental neutron activation analysis (INAA) using the procedures described by Sylvester *et al.* (1992). After neutron irradiation (151.75 h at a flux of 3×10^{14} n cm^2 sec^{-1}), the sample was counted 3x using two high-purity germanium detectors with efficiencies of 35.7% and 37.9%: for 22 h, 4.6 days after irradiation; for 2.0 days, 14 days after irradiation; and for 16 days, 64 days after irradiation. Interference corrections were made by procedures described by Sylvester *et al.* (1992). Blank corrections were <1% for Sm, Eu, Tb, Dy, Tm, Yb, Lu, Fe, Sb, Sc, Cr, Mo, Ru, As, and Na; 1–4% for La, Ce, Co, and Au; 6–15% for Ni, Ir, Os, and Zn; 31% for Se; and 49% for Ta. The results are given in Table 3.

Comparison of INAA results with the bulk chemical analysis (Table 1) is possible for five elements: Fe, Ni, Cr, Na, and Ca. The values for Fe and Na are in good agreement: Fe 11.02% (Table 1) and 10.80% (Table 3); Na 0.80% (as metal from Table 1) and 0.81% (Table 3). Calcium agrees within 10 relative percent: 1.64% (as metal from Table 1) and 1.48% (Table 3). This agreement indicates that the aliquot was representative of the bulk rock for the major phases making up the rock. Nickel and Cr by INAA (0.06% and 0.22%, respectively) are both low (within 50 relative percent) compared with the wet chemical analysis (0.13% and 0.34%, as metal, respectively). The Cr shortage may be due to less chromite in the aliquot analyzed by INAA because chromite is a minor phase in Watson and is not uniformly distributed. The low Ni content may be due to facts previously noted. Metal grains are a minor phase occurring inhomogeneously in the rock, and the Ni content of metal grains varies considerably from grain to grain. The conclusion we draw is that the INAA sample had somewhat less metal and chromite than the average whole rock.

For RNAA analysis, a 158-mg bulk sample was obtained from an interior fragment of Watson. Irradiation, radiochemical processing, counting, and data reduction were all obtained by the methods described by Wang and Lipschutz (1990). Chemical yields were 50–90% for all elements except Au (34%), Ag (28%), and Sb (28%). Chemical yields for monitors were 59–100%. Results are given in Table 3.

Comparison of RNAA and INAA data is possible for five elements: Co, Sb, Se, Zn and Au. Agreement for the first four of these elements is reasonable. Gold, however, is a factor of 10x higher in the INA analysis. As shown in Fig. 5, and discussed

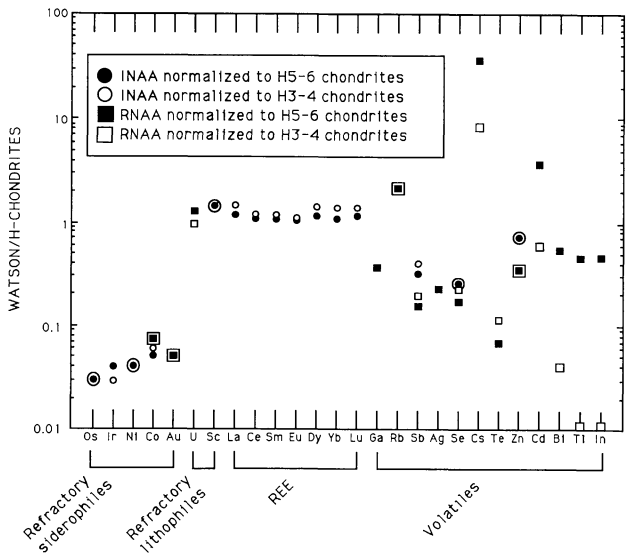

FIG. 5. Trace elements determined by INAA and RNAA. Solid and open circles are INAA values normalized to H4-6 and H3-4 chondrites, respectively. Solid and open squares are RNAA values normalized to H4-6 and H3-4 chondrites, respectively. If two values are close, they are plotted as a solid circle or square inside an open circle or square (see Table 3). Refractory siderophile, refractory lithophile and volatile elements are arranged in order of increasing volatility; REE are arranged by increasing atomic number.

TABLE 3. Watson Analyses by INAA (Sylvester & Grossman) and RNAA (Wang & Lipschutz)

ELEMENTS	INAA	RNAA	H5-6*		H3-4*	
MAJOR and MINOR						
Fe (%)	10.795±.0009	—	26.79±1.24	{31}	25.99±1.70	{22}
Ca (%)	1.48±0.04	—	1.23±0.08	{31}	—	{22}
Na (%)	0.8100±0.0170	—	0.60±0.09	{31}	—	{22}
Cr (%)	0.2173±0.0004	—	0.35±0.02	{31}	—	{22}
REFRACTORY SIDEROPHILE						
Os (ppb)	25.6±3.5	—	803±41	{4}	823±244	{6}
Ir (ppb)	29.2±0.9	—	798±49	{4}	853±256	{6}
Mo (ppm)	<3.0	—	—		—	
Ru (ppm)	<0.038	—	—		—	
Ni (%)	0.0629±0.0002	—	1.69±0.10	{31}	1.65±0.16	{22}
Co (ppm)	41.87±0.02	52.9	790±180	{58}	738±81	{11}
Au (ppb)	164±2	10.9	210±48	{26}	229±44	{6}
REFRACTORY LITHOPHILE						
U (ppb)	—	13.5	11±1	{4}	14±2	{6}
Sc (ppm)	9.972±0.001	—	7.7±1.4	{33}	7.4±1.3	{11}
Ta (ppb)	8.9±2.3	—	—		—	
RARE EARTH						
La (ppm)	0.414±0.006	—	0.328±.026	{4}	0.271±0.059	{3}
Ce (ppm)	0.953±0.013	—	0.855±0.060	{4}	0.755±0.117	{3}
Sm (ppm)	0.2166±0.0009	—	0.196±0.011	{4}	0.173±0.025	{3}
Eu (ppm)	0.0749±0.0016	—	0.0718±0.0026	{4}	0.0649±0.0092	{3}
Tb (ppm)	0.0598±0.0019	—	—		—	
Dy (ppm)	0.391±0.071	—	0.326±0.020	{4}	0.287±0.050	{3}
Tm (ppm)	0.0390±0.0016	—	—		—	
Yb (ppm)	0.242±0.007	—	0.210±0.012	{4}	0.183±0.032	{3}
Lu (ppm)	0.0406±0.0024	—	0.0331±0.0019	{4}	0.0307±0.0013	{2}
VOLATILE						
As (ppb)	<19	—	—		—	
Ga (ppm)	—	2.19	5.9±0.8	{55}	—	
Rb (ppm)	—	4.54	2.2 [1.5-3.3]	{58}	2.0±1.0	{6}
Sb (ppb)	24.5±0.1	11.6	77 [52-115]	{45}	62±11	{6}
Ag (ppb)	—	7.36	34 [16-71]	{58}	—	
Se (ppm)	2.02±0.01	1.39	8.1±1.2	{58}	6.3±1.4	{6}
Cs (ppb)	—	1110	32 [7-137]	{58}	130	{7}
Te (ppb)	—	24.7	360±120	{58}	230±177	{6}
Zn (ppm)	34.3±0.1	16.4	48±17	{58}	51±26	{6}
Cd (ppb)	—	18.3	4.8 [0.7-34.6]	{58}	31	{3}
Bi (ppb)	—	0.86±0.07	1.6 [0.5-5.3]	{58}	21	{11}
Tl (ppb)	—	0.15±0.02	0.33 [0.28-2.06]	{58}	14	{10}
In (ppb)	—	0.20±0.12	0.43 [0.13-1.48]	{58}	19	{8}

* Data from Lingner *et al.* (1987), Wolf and Lipschutz (1992), Morgan (1974), Rubin *et al.* (1980), Nakamura (1974) and Evensen *et al.* (1978).
Arithmetic means ±1 sigma; geometric means (Lipschutz *et al.*, 1983) when range is given.
Number of meteorites in { }.

later, all the siderophile elements are depleted in the Watson silicate mass, relative to H chondrites, due to the low abundance of metal. The RNAA value for Au is commensurate with the lower abundances of the other siderophile elements. We have examined the INA analyses carefully. Other samples in the same INA analysis group (principally CAIs) show expected Au contents. A previously analyzed standard in the group also gives its known Au content. We conclude that the Watson INAA sample was contaminated (probably by contact with gold jewelry) when it was chipped from the meteorite and not by subsequent processing. We have not included the INAA value for Au in Fig. 5, where it would have plotted one decade above the RNAA point. Finally, Dr. John Wasson (pers. comm.) has kindly provided us with his INAA results on Watson metal; the trace element concentrations lie within the IIE group.

Trace Element Compositions of Individual Minerals by Ion Microprobe

Trace elements in the silicate rock, including REE, were measured on grains of olivine, orthopyroxene, calcic pyroxene, feldspar and whitlockite (Table 4). These trace element data were collected with an AEI IM-20 ion microprobe using magnetic peak switching at low mass resolution ($M/\Delta M = 500$). Molecular interferences were suppressed by energy filtering. Calcium-normalized ion yields and interferences were determined from a variety of silicate minerals and glasses. Silicates and phosphates are known to have similar Ca-normalized ion yields (Zinner and Crozaz, 1986; Fahey *et al.*, 1987).

The close-packed structure of olivine precludes accommodation of large ion lithophile (LIL) elements such as REE, except in Ca-rich olivine in refractory inclusions (Davis *et al.*, 1991). The low-Ca olivine in Watson is characteristically very depleted in LIL elements. The REE enrichment factors relative to C1 chondrites are, therefore, plotted for low- and high-Ca pyroxene, feldspar and whitlockite in Fig. 6.

In Fig. 6, the REE patterns for the pyroxenes and feldspar are fairly typical of these phases for chondritic bulk compositions. The whitlockite pattern is, however, remarkable. Relative to C1 chondrites, phosphates in H-chondrites generally have fairly uniform light rare earth element (LREE) enrichments of ≈300 and heavy rare earth element (HREE) enrichments that drop from ≈300 for Gd to 100–150 for Lu (Crozaz *et al.*, 1989). In contrast, Watson whitlockite has LREE enrichments that drop steadily from 720 for La to 300 for Sm and HREE enrichments that continue the drop to 90 for Lu.

Table 4. Ion microprobe analyses of individual phases in the Watson silicate inclusion. Oxide concentrations are in wt% and are given only for oxides with concentrations of > 1 wt%. Elemental concentrations are in ppm. Uncertainties due to counting statistics are given only when they exceed 10% of the amount present. (A. Davis, analyst)

	Olivine	Orthopyroxene	Clinopyroxene	Feldspar	Whitlockite
Na_2O				9.0	1.9
MgO	40	29	20		
Al_2O_3			1.2	20	
SiO_2	38	56	52	68	
K_2O				1.7	
P_2O_5					45
CaO		1.0	17		52
Cr_2O_3			1.3		
FeO	21	12	7.1		1.6
Li	1.9	2.5	0.96	0.13±0.03	
Be	0.17±0.04	0.13±0.03	0.18±0.05	0.48±0.08	
B	0.13±0.05	0.38±0.09	0.21±0.08	1.3	
Na	23	622	4093		
Mg				1899	
Al	52	1835	6277		
K	4.6	3.6	92		
Ca	188	7449		5473	
Sc	3.0±0.4	9.0	50	<1.6	
Ti	106	378	1583	513	
V	7.1±4.9	62	279	7.4±1.6	
Cr	455	4568	9103	70	
Mn	3503	3547	2557	<57	
Rb	<1.3	<1.0	<1.0	55	<2.4
Sr	0.23±0.05	0.15±0.04	6.2	33	105
Y	0.16±0.04	1.1	8.7	0.16±0.05	165
Zr	0.29±0.07	0.27±0.07	2.5	1.2±0.2	6.3±1.1
Nb	0.12±0.05	0.06±0.03	0.76±0.14	0.54±0.12	1.0±0.4
Cs	0.07±0.05	0.18±0.07	<0.09	6.2	<0.7
Ba	0.033±0.026	0.029±0.023	0.25±0.08	30	52
La	0.067±0.012	0.017±0.006	0.27±0.03	0.85	169
Ce	0.037±0.014	0.015±0.009	1.2	0.58±0.07	399
Pr	<0.030	<0.016	0.31±0.06	0.038±0.024	50
Nd	<0.062	<0.068	1.3±0.2	0.27±0.10	201
Sm	<0.016	0.028±0.012	0.62±0.06	<0.082	44
Eu	<0.0060	<0.0060	0.060±0.012	0.27±0.04	2.0±0.2
Gd	<0.056	0.057±0.028	1.2±0.2	<0.078	39±5
Tb	<0.010	0.016±0.008	0.25±0.04	<0.012	5.1±0.9
Dy	<0.028	0.15±0.03	1.5	<0.044	38
Ho	<0.022	0.040±0.014	0.35±0.05	<0.018	6.9±0.7
Er	<0.028	0.092±0.022	0.86	<0.044	22
Tm	<0.0047	0.035±0.009	0.13±0.02	<0.018	3.5
Yb	<0.036	0.16±0.04	0.61±0.10	<0.044	18
Lu	<0.0089	0.025±0.008	0.12±0.03	<0.0010	2.1±0.5
Hf	<0.022	<0.036	0.19±0.07	<0.068	<2.5
Th	<0.010	<0.013	<0.014	<0.016	3.9±0.5
U					1.1±0.2

One similarity between Watson and H-chondritic whitlockite is that both have Eu enrichments that are 10x lower than those expected from interpolation between Sm and Gd.

Armstrong *et al.* (1990) analyzed REE in an apatite from a silicate inclusion in the IIE iron meteorite Colomera. That apatite shows a small enrichment (by about 8x) of HREE over LREE, the reverse of the trend measured in Watson whitlockite. Colomera apatite has REE enrichments that are somewhat irregular, no significant Eu anomaly and an extraordinary 20x negative Yb anomaly. Apatite in equilibrated H-chondrites has C1 chondrite-normalized enrichments that drop steadily from ≈60 for La to ≈12 for Lu; they do not have significant Eu or Yb anomalies (Crozaz *et al.*, 1989).

Whitlockites in KREEP-rich lunar rocks show enrichments of LREE over HREE, as in Watson whitlockite, but the patterns are not as steeply fractionated. Watson whitlockite has a C1 chondrite-normalized La/Yb ratio of 6.5, whereas this ratio is ≈2.7 in lunar whitlockite analyzed by Snyder *et al.* (1992). Lunar whitlockites show deep negative Eu anomalies (Lindstrom *et al.*, 1985).

We calculated a whole rock REE pattern by combining the modal analysis with REE data for individual phases. The resulting pattern is LREE-enriched, with C1 chondrite-normalized enrichment factors of 10 for La, 3.9 for Sm and 2.0 for the HREE Dy to Lu. In this calculation, we assumed that the whitlockite analysis is representative of phosphate in the silicate portion of Watson. The disagreement between our calculated REE pattern and that measured by INAA (Fig. 6) shows that this assumption is not correct. The P_2O_5 content of Watson must be dominated by the P-rich stringy interstitial material described earlier, and this material must be substantially lower in REE than the whitlockite we analyzed by ion microprobe

Noble Gas Analyses

The isotopic compositions and concentrations of He, Ne and Ar have been measured in both metal and silicates of Watson. Sample weights were 85 and 121 mg, respectively. Apparatus and experimental procedures were the same as described by Schultz *et al.* (1991). The results are in Table 5.

Metal—All noble gas isotopes in Watson metal are cosmogenic (*i.e.*, produced by galactic cosmic rays during the flight of the meteoroid in space). Some of the ^{40}Ar is due to adsorbed Ar from the terrestrial atmosphere or to a small but significant contamination with silicate material. The systematics

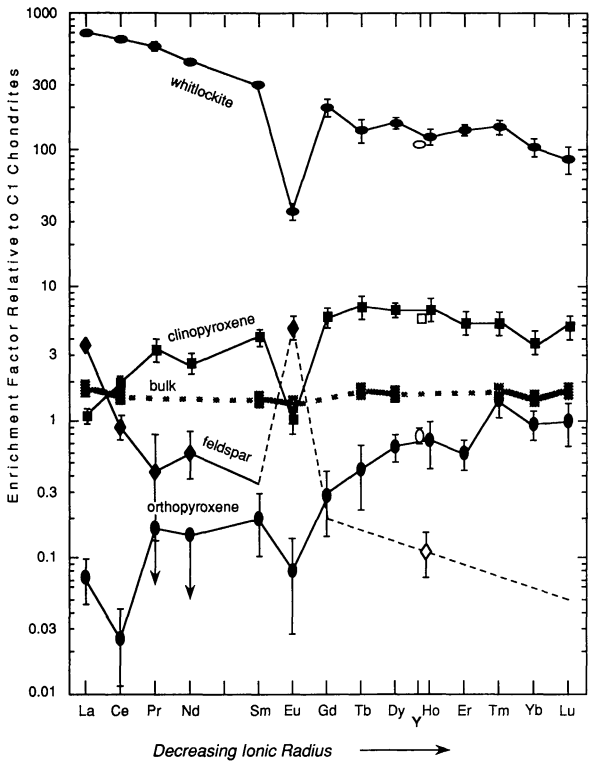

FIG. 6. REE (and Y) concentrations in Watson minerals determined by ion microprobe. Whole rock REE determined by INAA. All data normalized to C1 chondrites. Compare Fig. 5 for REE normalized to H-chondrites.

of cosmogenic noble gas nuclides in iron meteorites has been summarized by Voshage (1982). The cosmogenic nuclide ratios of the isotopes ^{4}He, ^{21}Ne and ^{38}Ar follow these correlations. For ^{3}He, however, a deficit of about 15% is observed. Such a deficit has been found in many hexahedrites (Hintenberger *et al.*, 1967) and also in other iron meteorite groups (*e.g.*, Schultz, 1967). This deficit of ^{3}He is explained by solar heating in space and loss of tritium, a progenitor of ^{3}He (Buchwald, 1971).

Gas Retention Ages of Silicates—The noble gases of the silicate rock inclusion are a mixture of radiogenic (subscript r) ^{4}He$_r$ and ^{40}Ar$_r$, cosmogenic gases (subscript c) and a small trapped component of Ar, Kr and Xe. Assuming that ^{4}He = ^{4}He$_r$ + ^{4}He$_c$ and that ^{4}He$_c$ = 5 x ^{3}He$_c$, ^{4}He$_r$ can be calculated. Using the determined RNAA U concentration (Table 3) and the Th/U ratio of 3.5, which is the value for average H-chondrites, a ^{4}He-U, Th gas retention age can be calculated, as well as a model K-Ar age using the measured ^{40}Ar concentration and a K concentration of 0.23 wt% (Table 1). These gas retention ages are given in Table 6. The K-Ar age, 3.5 ± 0.2 Ga, is closer to the Rb-Sr age of the silicate inclusions in the IIE iron meteorite Kodaikanal, 3.7 ± 0.1 Ga (Burnett and Wasserburg, 1967) and the ^{40}Ar-^{39}Ar age of Netschaëvo, 3.8 Ga (Niemeyer, 1980), than it is to other dated IIEs, Colomera, 4.61 Ga (Sanz *et al.*, 1970) and Weekeroo Station, 4.54 Ga (Niemeyer, 1980).

The ^{4}He-U, Th age, 3.1 ± 0.3 Ga, is shorter but within error of the K-Ar age. Because of the ease of He loss, this age would be expected to be shorter especially if, as will be discussed later, a later shock event took place which caused the release of the Watson mass into interplanetary space. The 3.5 Ga age indicates that Watson has not experienced a major pervasive thermal event since that time.

Exposure Ages—From the concentrations of cosmogenic ^{3}He, ^{21}Ne and ^{38}Ar of the silicate rock, cosmic-ray exposure ages can be calculated if the respective production rates are known. These rates can be calculated from the chemical composition of the silicates. A correction for shielding, however, is not possible because the chondritic relationship between irradiation hardness and production rate does not hold in iron meteorites. This is immediately apparent from the cosmogenic ^{22}Ne/^{21}Ne ratio of 1.039 ± 0.004, which is significantly lower than the lower limit of 1.06 found to hold for chondrites (Begemann *et al.*, 1985 and pers. comm.); for a very highly shielded chondrite, a value as low as 1.05 might be found. It reflects enhanced production of ^{21}Ne *via* ^{24}Mg (n,α) in silicate inclusions within iron and stony-iron meteorites. This effect has been studied in stony-iron meteorites (Begemann *et al.*, 1976; Begemann and Schultz, 1988) and is caused by a higher flux of secondary particles in materials composed mainly of elements with higher atomic number (Fe and Ni). The influence of this effect on the absolute production rate of neon is not yet known.

Using production rates as deduced from H-chondrites and representative for a shielding characterized by ^{22}Ne/^{21}Ne = 1.11 (Eugster, 1988), shielding-uncorrected exposure ages of the silicate rock are calculated and given in Table 6. The above described matrix effect would result in higher production rates for Ne. The good agreement of all these exposure ages indicates that this effect should not enhance the Ne production rate by

Table 5. Noble gas concentrations in the metal and the silicate inclusion of the Watson meteorite (10^{-8} cm^3 STP/g)

	Metal	Silicate
^{3}He	9.23 (10.89)*	13.70
^{4}He	37	1295
^{20}Ne	0.138	2.97
^{21}Ne	0.154	3.31
^{22}Ne	0.166	3.44
^{36}Ar	0.41	0.71
^{38}Ar	0.66	0.42
^{40}Ar	1	9130
^{84}Kr	-	0.026
^{132}Xe	-	0.003

* ^{3}He deficit corrected (*cf.* text)

Table 6. Gas retention ages and exposure ages of Watson metal and silicate inclusion

	Gas retention ages (in Ga)		Exposure Ages (in Ma)		
	^{4}He-U-Th	K-Ar	^{3}He	^{21}Ne	^{38}Ar
Metal				>10.5*	7.7**
Silicate	3.1	3.5	8.2	8.5	7.9

* According to Voshage (1984)

** Using a production rate of 0.086x10^{-8} cm^3 STP ^{38}Ar/g$_{Fe}$ Ma (Begemann et al, 1976)

more than about 20% over those of ^{3}He or ^{38}Ar. Also, the cosmogenic ^{10}Be and ^{26}Al concentrations in the Watson silicate mass were measured by Herzog and Xue (pers. comm.): 24.3 ± 0.8 dpm/kg and 69.3 ± 2.3 dpm/kg, respectively. These are normal values if the lower bulk Fe content of whole rock Watson silicates relative to average H-chondrites is considered. Taking everything into account, an exposure age for the silicate mass of 8 ± 2 Ma should include the uncertainties introduced by this matrix effect.

Voshage (1984) has given a range of production rates for ^{4}He, ^{21}Ne and ^{38}Ar for a given shielding characterized by $^{4}He/^{21}Ne = 240 \pm 10$ in Fe metal; from these rates, we are able to calculate a range of possible exposure ages of the metal. With the maximum production rate of these nuclides (including their uncertainties), we calculate the shortest possible exposure age of 10.5 ± 0.5 Ma. Using Voshage's lowest possible production rate, we estimate the longest possible exposure age of approximately 30 Ma. Using the production rate of ^{38}Ar, as deduced by Begemann *et al.* (1976) from H-chondrites for metal, an exposure age of 7.7 Ma is obtained, which is in good agreement with the 8 Ma value for the silicate portion of Watson. G. Herzog and S. Xue (pers. comm.) have measured cosmogenic ^{10}Be and ^{26}Al in Watson metal: 5.2 ± 0.5 dpm/kg and 3.6 ± 1.3 dpm/kg, respectively. These values are normal for small iron meteorites.

In terms of these exposure age calculations, there is no significant difference in the exposure age of Watson silicate and Watson metal. The apparent difference that does show up, 10.5 *vs.* 8 Ma, is caused by the use of two sets of production rates: that derived from stone meteorites (1–100 Ma exposure ages) and that derived from iron meteorites (exposure ages >100 Ma). The reason for the difference in production rates could be due to a change in cosmic ray intensity which took place between these two time intervals, as hypothesized by several workers (Voshage, 1962; Hampel and Schaeffer, 1979).

Most iron meteorites have exposure ages of several hundreds of millions of years (Fig. 7). Exposure age data for other IIE iron meteorites are sparse. Vilcsek and Wänke (1963) obtained an exposure age of 75 Ma for Colomera based on measurement of ^{36}Cl. Noble gas measurements on Weekeroo Station and Arlington IIE iron (the latter has no reported silicate inclusions) imply much longer exposure ages than that of Watson, an estimated 600 Ma and 300 Ma, respectively. New noble gas measurements on Netschaëvo have been completed. Because Netschaëvo has been artificially heated, the results are less firm than desired. Nevertheless, it appears to have a shorter exposure age than that of Watson, between 2 and 4 Ma. Exposure age data for Kodaikanal are also inadequate to calculate a firm exposure age, but an estimate can be made of ~4 Ma.

The exposure age of Watson is, within the limits of error, equal to the 8 Ma exposure age cluster of H-chondrites that contains about 45% of all H-chondrites (Fig. 7) and dates the time of an impact event sufficient to release Watson into interplanetary space. The agreement of the exposure ages of this cluster and of Watson is another link between this iron meteorite and the ordinary H-chondrites.

Trapped Gases in Silicates—Trapped Ar, Kr, and Xe in ordinary chondrites correlate with the chemical-petrographic type of the meteorite (Zähringer, 1966; Marti, 1967; Schultz, 1990). Compared to type 5 or 6 ordinary chondrites, the concentration of these components in the Watson silicate inclusion is small, only about 60% of the values common in those chondrites. For example, ^{132}Xe of type 5 and 6 ordinary chondrites is normally greater than 0.005×10^{-8} ccSTP/g; in Watson silicate it is 0.003 x 10-8 ccSTP/g. Krypton, however, is higher than expected. The relatively high $^{84}Kr/^{132}Xe$ ratio, 8.7, as well as the $^{129}Xe/^{132}Xe$ ratio of ≈1, are together indicative of adsorbed gases from the terrestrial atmosphere. Thus, the silicate melting event in Watson, as inferred from petrographic observations has removed most planetary type gases.

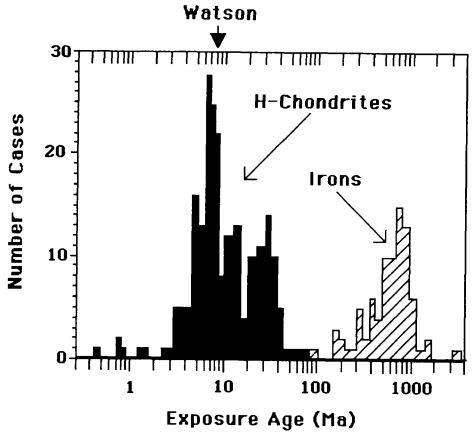

Fig. 7. Cosmic ray exposure age distribution of H-chondrites and iron meteorites on logarithmic scale. The resolution is 20% of the age. To avoid uncertainties due to insufficient shielding corrections, only ages of H-chondrites with $^{22}Ne/^{21}Ne \geq 1.08$ are taken (data from Schultz and Kruse, 1989, and other later unpublished data). Data for iron meteorites are from Voshage and Feldman (1979) and Voshage *et al.* (1983). The exposure age of Watson, marked by an arrow, is at the mode of the major H-chondrite cluster at about 8 Ma.

INTERPRETATION OF OBSERVATIONS

The most reasonable interpretation of the petrographic evidence and the bulk wet chemical analysis is that Watson silicate is an H-group chondrite that melted and was incorporated as an immiscible mass within molten IIE metal (temperature = >1550 °C). The system remained hot long enough to melt the silicate mass entirely (although some crystal nuclei may have persisted). Most of the chemical and mineralogical characteristics of a chondrite are preserved except for the loss of chondritic texture and of metal and sulfides, leaving it with a low metal igneous texture. The flat REE pattern (Fig. 5) indicates that melting took place without significant fractionation of silicates. The REE pattern, however, shows a small enrichment of every REE measured above that of either average H3-4 or H5-6 by factors of 1.04 to 1.53 (Fig. 5) but within the range of variation known for H-chondrites. The bulk K_2O content is 2x higher than average H-group chondrites (Table 1) although the Na/K molar ratio in Watson is 6, which is just within the observed chondrite range, 6 to 17 (Jarosewich, 1990). This ratio is also 6 in the chondrule-bearing silicate masses of the IIE meteorite Netschaëvo. Netschaëvo silicate is close to H-group chondrite compositions, but somewhat different. Olsen and Jarosewich (1971) stated that Netschaëvo silicate is "more H than H". Bild and Wasson (1977) later established that the Netschaëvo silicate rock is sufficiently distinct from most H-group chondrites to define a new group,

the HH-chondrites. This is supported by the oxygen isotope composition of Netschaëvo ($\delta^{17}O$ = +2.37, $\delta^{18}O$ = +3.46‰); it lies close to, but somewhat off, the fractionation line that runs through the H-group chondrites and the silicates of the IIE iron meteorites. Also, Olsen and Jarosewich (1971) determined that the ratio of modal olivine/(olivine + pyroxene) in Netschaëvo is 0.31, which differs significantly from the H-group chondrites, which range from 0.43 to 0.67; this value for Watson is 0.67. Bunch *et al.* (1970) did not find any olivine in the IIE irons Weekeroo Station and Colomera and only trace amounts in Kodaikanal. Osadchii *et al.* (1981) reported that olivine is an accessory phase in Elga. Bild and Wasson (1977) showed that Netschaëvo plots along an extension of a curve which passes through the L and H chondrites in an oxidized *vs.* reduced Fe diagram. Watson silicate mass has very little metal and cannot be plotted on this diagram. It appears that during melting, the metal and troilite in the original H-chondrite mass formed immiscible blebs of Fe-FeS eutectic that migrated to the surrounding metal interface.

The analyses of trace elements determined by INAA and RNAA in Watson are listed in Table 3. It was possible to normalize many of the trace elements against average literature values for H4-6 chondrites and, in five cases, for H3-4 falls (Evensen *et al.*, 1978; Lingner *et al.*, 1987; Wolf and Lipschutz, 1992; Rubin *et al.*,1980; Morgan *et al.*, 1985). The normalized values are plotted in Fig. 5.

Refractory siderophile elements are significantly depleted due to the loss of metal from the silicate mass. Refractory lithophile and rare earth elements are present at average H-chondrite concentrations. The REE pattern is essentially flat at ≈1 x H (or 1.6x C1 chondrites).

The volatile elements offer a more complicated picture. The volatile elements Ga, Sb, Ag, Se, Zn, Cd, Bi, Tl, and In are all depleted by comparable amounts, 0.2 to 0.8 of H-chondrites, the magnitude presumably controlled by the respective distribution coefficients into the sulfide melt. Some of these are strongly chalcophile and reflect the loss of troilite. Where both INAA and RNAA data sets overlap for the volatile chalcophile elements, the INAA value is higher than that for the larger RNAA sample, which apparently had a troilite content closer to the bulk. This suggests that the INAA sample had somewhat more sulfide than representative of the bulk. As noted earlier, the INAA sample is clearly representative of the bulk rock for the major elements, but elements concentrated in the inhomogeneously distributed minor phases, metal, chromite and troilite may not be representative of the whole in the small sample that was used for analysis. Gallium, within the Watson silicate mass, would be lithophile. It also has chalcophile affinities under more reducing conditions. It may have been lost to the surrounding metal as a vapor and entered into the sulfide phase.

The volatile lithophile elements, Rb and Cs, are both enriched above average H-chondrite values, Cs by an extraordinary amount. Both these elements are known to substitute into the feldspar structure; their increased concentrations go along with the observation that Watson silicate contains about twice the average K content of normal H-chondrites, physically reflected in the presence of antiperthite and a high modal Or content. The magnitude of the Cs enrichment, however, defies explanation. Similarly, the chalcophile element, Cd, is unusually enriched. Because Watson is a find, it is possible Cd enrichment is due to terrestrial contamination. Although if that were the case, we would expect an even larger enrichment in Zn, which accompanies Cd geochemically. Also, Cd is very mobile and could have entered the silicate mass from the surrounding metal.

In Fig. 5, five data for volatile trace elements (Cs, Cd, Bi, Tl, and In) were normalized against literature values for H3-4 falls. In each case, the depletion is considerably greater than for the higher petrographic grades.

From the refractory lithophile and REE, it is clear that the silicate phases in the original Watson chondrite mass melted under relatively closed conditions. This supports the conclusion drawn from the major and minor elements (Table 1). The factor of two enrichment of K, relative to average H-chondrites, is still within the upper range of K values known in H-chondrites. The factor of two enrichment of phosphate, however, is outside the range of values for known H-chondrites. To make certain of this value (Table 1), whole rock P was re-analyzed two additional times (a total of three times); each time, the same value was obtained. Phosphate could easily have been introduced into the silicate mass from partial oxidation of P, or phosphide, in the surrounding metal during the melting event.

Two mineralogical thermometers can be applied to the silicate mass in Watson: the two-pyroxene (PX-PX) thermometer of Lindsley (1983) and the olivine-spinel (OL-SP) thermometer of Sack and Ghiorso (1991). When these two thermometers are applied to a wide variety of meteorite groups, the equilibration temperature registered by OL-SP is lower than that of the PX-PX thermometer by several tens of degrees to several hundreds of degrees (Olsen, unpublished data). This indicates that cation exchange between olivine and spinel continues to lower temperatures after the exchange between coexisting pyroxenes has essentially ceased. The magnitude of the differential between the two temperatures in each case depends on differences in the cooling histories. We know from the ordinary chondrites that the PX-PX thermometer in meteorites is capable of recording equilibration temperatures as low as 800 °C (Olsen and Bunch, 1984). In terrestrial rocks, this thermometer records even lower temperatures, 550°–600 °C (Lindsley, 1983), but terrestrial rocks always contain some water which facilitates equilibration to lower temperatures than in the dry environment of equilibrated ordinary chondrites. The OL-SP thermometer can register a temperature down to 700 °C in some meteorites (Olsen, in prep). For the purposes of discussion here, we shall consider 800 °C and 700 °C as essentially the closure temperatures of the PX-PX and OL-SP thermometers, respectively, in dry meteorites. It is possible that lower temperatures will be discovered as more meteorites are examined.

Applying these two thermometers to Watson, we obtain 1100 °C for both thermometers. We conclude that this high temperature and the lack of a temperature differential between the two thermometers in Watson indicate that the silicate mass cooled quickly after the event which heated it to a temperature higher than 1100 °C. The metallography of the host Fe also reveals a great deal about the cooling history. We will return to the question of the entire cooling history later in this paper.

The earliest event in the making of the structure of Watson was that of molten metal engulfing an H-chondrite mass. Silicate melted, and chondritic texture was lost. Metal grains within the chondrite reacted with troilite and melted, forming immiscible droplets of Fe-FeS eutectic, most of which migrated to the surrounding metal contact. Small amounts of silicate

material were apparently squeezed into surrounding metal as immiscible blebs. These became "pinning" points on which taenite later nucleated in the metal. There are some features of the mineral chemistry of the isolated silicate blebs that suggest the original chondritic silicates were not completely equilibrated with each other before metal-silicate mixing. Within the main silicate mass and within each isolated silicate bleb, mineral grain compositions are now individually uniform, but there are notable differences between the main silicate mass and some blebs. These could have arisen if unequilibrated chondritic material were invaded by molten metal, and small detached blebs were isolated in the metal. Each separate bleb and the main silicate mass melted completely and then crystallized, giving internally homogeneous chemical compositions for constituent minerals. This could explain the observed small differences in olivine and pyroxene mineral compositions in the two sitings. The mineral chemical differences among feldspars, however, remain puzzling. Feldspar in silicate blebs is much more calcic (An_{45-54}) than any feldspar composition observed in the silicate mass, yet Ca-rich feldspar is only found in the most unequilibrated H-chondrites. If an unequilibrated chondrite were disrupted by molten metal, we would expect to find at least some more albitic feldspar in the silicate blebs isolated in metal. No albitic feldspar was found in seven blebs we were able to analyze. At the present time, we cannot account for these observations. Because the occurrences of feldspathic material as isolated blebs in metal are so few, it is possible that future studies of the metal will reveal broader composition variations and more albitic feldspar will be discovered, confirming the possibility that the original Watson chondrite was of low petrographic grade, H3-4.

The last event that is recorded in the melting of the original Watson chondrite mass was cooling to 1100 °C, which is recorded by both mineral thermometers.

The polycrystalline taenite structure of the surrounding metal constrains the cooling history. Cooling from 1100 °C to below 800 °C must have been relatively rapid, otherwise, the polycrystalline taenite would have transformed into a large single crystal. Structural development in the metal from 800° to 550 °C can be modeled using the Fe-Ni-P equilibrium diagram as was done for coarse structured iron meteorites by Clarke and Goldstein (1978); this model is applicable to other classes of iron meteorites as well. Sulfur does not affect this model because by 800 °C it has all been removed as troilite. Table 7 summarizes changes in atom% of kamacite (α), taenite (γ) and schreibersite (Ph) with decreasing temperature as well as changes in their chemical compositions as reflected by Ni content. The assumed starting composition is 8.2 wt% Ni, 0.5 wt% P with the remainder being Fe. The P content is increased slightly over the analytical value of 0.38 wt% to 0.5 wt% to compensate for the presence of large schreibersite crystals that were avoided in the selection of samples for bulk analysis. Polycrystalline taenite constituted the metallic mass down to about 800 °C (Table 7, col. 3). By 750 °C, about half of the volume of schreibersite had precipitated probably mainly at taenite-taenite grain boundaries. At somewhat lower temperatures, kamacite began to precipitate, initially at interfaces with schreibersite and possibly also at taenite-taenite grain boundaries. By 700 °C, approximately 15% of the structure had been converted from taenite to low-Ni kamacite and low-Ni schreibersite. With continued cooling, kamacite increased in volume and Ni content, and schreibersite increased in Ni content. From ~600 °C, schreibersite increased both in amount and Ni content. By 500 °C, the macroscopic structure seen in undisturbed metal areas had formed.

Metallographic examination on a finer scale indicates that the growth process continued to below 300 °C. Electron microprobe analysis gave taenite nickel concentrations of 26 wt% at borders of plessite areas with surrounding kamacite. The taenite crystals are very narrow and, under these circumstances, the true interface Ni concentration is undoubtedly higher. A 56-μm wide schreibersite had a Ni concentration of 31 wt%. These Ni concentrations in taenite and schreibersite indicate WP growth to temperatures well below 550 °C.

Nickel concentrations in kamacite away from other phases range from 7.6 to 7.8 wt%. The Ni concentration in kamacite at the interface with the schreibersite mentioned above was 5.6 wt% with a smooth decline from bulk kamacite values over a distance of at least 50 μm. There was also about a 0.5 wt% depression in the Ni value at the interface with taenite surrounding plessite fields. These are values to be expected for a relatively undisturbed WP that developed at cooling rates substantially faster than the maximum of 5 °C/Ma among meteorites studied by Clarke and Goldstein (1978). Iron meteorites which have cooled more slowly have lower bulk Ni concentrations for kamacite.

From the metallographic examination alone, it is difficult to arrive at an accurate estimate for the cooling rate of Watson through the WP growth range. It was undoubtedly fast compared to many other kinds of iron meteorites. Bristol, a IVA meteorite, has kamacite band widths about twice that of Watson, along with certain structural similarities and similar bulk Ni and Co contents, but with significantly lower P content (Buchwald, 1975). Saikumar and Goldstein (1988) proposed a cooling rate of 150–300 °C/Ma for Bristol. Watson has narrower kamacite bands and much more P, both of which speak for a considerably faster cooling rate than that of Bristol. Although much has changed since Bence and Burnett (1969) estimated an average cooling rate of ≈1000 °C/Ma for Kodaikanal, it may well prove to be an appropriate estimate for both Kodaikanal and Watson. We will adopt that figure here.

During the period when the metal was undergoing the transformations just described, small chemical adjustments were taking place in the silicate mass: compositional zoning of minerals due to magmatic crystallization was homogenized; exsolution in feldspar (antiperthite) and Ca pyroxene must have occurred. As stated earlier, it is not possible to determine directly the average bulk feldspar composition in Watson

TABLE 7. Equilibrium cooling of a composition appropriate for the Watson meteorite. Atomic percentage of phases present at the indicated temperatures with their Ni contents.

Starting composition:		7.8 atom% Ni, 0.9 atom% P (8.2 wt% Ni, 0.5 wt% P)				
T°C	α	γ	Ph	Ni(α)	Ni(γ)	Ni(Ph)
850		100.0			7.8	
750		98.7	1.3		7.8	5.8
700	14.2	84.5	1.3	4.3	8.4	7.1
650	60.4	38.6	1.0	5.1	12.0	9.0
600	79.0	19.5	1.5	5.9	15.1	12.8
550	90.5	7.4	2.1	6.6	20.2	16.0

because of the variability in composition of the cloudy feldspar and the variable density of K-feldspar exsolution lamellae in clear, well-crystallized feldspar. It was, however, possible to calculate a bulk feldspar composition of approximately $An_{10}Or_{13}$. The known solvi for alkali feldspars (Parsons, 1978) peak at about 650 °C (at the composition An_0Or_{35}). This would be the upper temperature limit for antiperthite exsolution, although we cannot determine the exact temperature because the solvi apply to Ca-free alkali feldspars. This exsolution is a kinetically slow process, especially in a dry system. It had to have taken place during the cooling interval in which the surrounding metal structures formed. It could not have taken place during quench cooling after a shock event (J. R. Goldsmith, pers. comm.). The same can be said for slow exsolution rates determined in the Ca pyroxenes (Ross *et al.*, 1969).

The noble gas retention age, 3.5 Ga, provides a chronology for the whole process up to this point. The metal-silicate melt formation was initiated by an unknown cause, most likely by a major impact event at some time just prior to 3.5 Ga. Initial cooling and nucleation of phases in the metal and the silicate masses took place down to the 1100 °C temperature recorded by both of the mineralogical thermometers. By this time, the silicates were able to retain noble gases. The relatively small size of the taenite crystals and the freezing in of the OL-SP thermometer at 1100 °C suggest that the cooling rate must have increased below ≈1100 °C. Thus, from 3.5 Ga to some time long before 8 Ma ago, the whole system finally cooled to a temperature below 300 °C at an overall average rate estimated to be 1000 °C/Ma.

The shock event that is so prominently recorded in Watson metal took place after all the solid structures had formed. The phosphide melt pockets in the metal, described above, are the extreme expression of this event. These numerous P-rich melt pools were formed when localized shock pressure focused on some schreibersite grains and raised their temperatures sufficiently to melt them. The melted schreibersite reacted with surrounding metal, incorporating several times its volume into the pocket. For example, the melt pocket in Fig. 3 may be approximated by a sphere 1.8 mm in diameter. The 3 wt% P concentration measured in this melt pocket is 20% of that expected for schreibersite, indicating that 20% of the present volume of the pocket was occupied by schreibersite. A 1 mm diameter spherical schreibersite with a Ni content of 17 wt% would explain the observed pool with 80% of the pool due to melted metal.

The occurrence of such large melt pockets in close proximity to essentially undisturbed WP might seem unreasonable. The dendritic structure of the melt products, however, provides an explanation. The melt pockets quenched at an extremely high cooling rate, indicating a steep thermal gradient into the surrounding metal that must have been cold enough to provide an effective heat sink. Dendrite arm spacing for similar quenched melts was used by Blau *et al.* (1973) and Scott (1982) to determine cooling rates and was applied by Bevan *et al.* (1979) and Buchwald and Clarke (1987) to determine melt pocket cooling rate for the Verkhne Dnieprovsk meteorite. Arm spacings are somewhat less distinct in the Watson section than they were in Verkhne Dnieprovsk, but they are clearly very close to the 2 μm value given by Buchwald and Clarke (1987), who determined a quench rate of 10^4 to 10^5 °C/s. The smaller the dendrite arm spacing, the faster the cooling rate. The shock event caused this distortion to the structure and locally developed high enough temperatures to melt schreibersite and a comparatively large volume of surrounding metal and to transform neighboring kamacite into α_2. Most of the metal structure, however, was little affected. Within the silicate mass, the shock event appears to have physically affected primarily the feldspar. The cloudy feldspar occurrences are almost certainly the result of shock deformation, which sheared and heated pre-existing feldspar. The clearer feldspars associated with cloudy feldspar must represent unaffected pre-shock feldspar. The event was too fast and localized to affect the mineral thermometers and exsolution lamellae. This shock was very probably the breakup event which released Watson into interplanetary space 8 Ma ago. The model K-Ar age of the silicate inclusion in Watson, about 3.5 Ga, is comparable to ages measured for Kodaikanal and Netschaëvo silicates.

INFERENCES AND SPECULATIONS

Netschaëvo

As stated earlier, the silicate inclusions in the Netschaëvo iron meteorite are not exactly true H-group chondrite material (Bild and Wasson, 1977). Also, as noted earlier, the bulk oxygen isotope composition of Netschaëvo lies close to, but not on, the fractionation line that passes through the H-chondrites and the silicate inclusions of the IIE iron meteorites in the three oxygen isotope diagram (Clayton *et al.*, 1983). Nevertheless, some inferences can be made about this meteorite based on some of the conclusions we have been able to draw about Watson.

The silicate material in Netschaëvo must have initially come into contact with metal which caused the chondrite mass to be brecciated into the angular fragments we now see (Fig. 1238 in Buchwald, 1975), each being engulfed by metal. Cooling must have been extremely rapid initially to preserve chondrules and not cause extensive melting as seen in Watson.

Kodaikanal

The similarities between Watson and Kodaikanal are remarkable. The globular inclusions in Kodaikanal contain olivine and low-Ca pyroxene with compositions, Fa_{21} and Fs_{17}, respectively, identical to those in the Watson silicate mass. Kodaikanal feldspars are relatively K-rich, as are the feldspars in Watson. The metallographic structure of Kodaikanal is very much like that of Watson metal and indicates a similar cooling history in the range below 800 °C. Metal distortion due to later shock in Kodaikanal is not quite as severe as that in Watson, and no melt pockets were created by the process.

Although Kodaikanal and Watson exhibit similar metallurgical histories, the silicate inclusions in Kodaikanal are more complex. The silicates in Kodaikanal were introduced in larger quantities into the metal than in Watson, after their source rock had evolved to a fractionated state. The Watson silicate mass represents the first step in the creation of the globular silicate masses seen in Kodaikanal and such other IIE iron meteorites as Elga, Weekeroo Station, and Colomera. Prinz *et al.* (1983) determined that the mineralogy of the globular silicate inclusions in most IIEs, which Armstrong *et al.* (1990) called "rhyolitic plums," is a minimum melt composition and must have been preceded by an igneous fractionation process. This could have been accomplished in one stage or in a series of stages in which original chondritic masses were engulfed in metal (such as those in Netschaëvo), melting took place (such as in Watson), followed by fractionation (as in

Kodaikanal). Some of the final liquid/solid fractionated material was squeezed into the surrounding Kodaikanal metal. In the fractionated cases, such as Kodaikanal, this process must have left behind a complementary olivine-rich silicate fraction.

Planetary Processes

Wasson and Wang (1986) proposed that IIE irons formed by impact melting of metal and silicate near the surface of a chondritic parent body, based on the fact that interelement relationships among the siderophile elements in the metal are like those found in other nonmagmatic Fe groups (such as IAB) rather than those found in magmatic Fe groups (like IIIAB). Taylor (1991) showed that asteroids will not form cores unless >70% melting of silicates occurs, because high interfacial energies between metal and silicate prevent the formation of an interconnected metallic melt and because silicate mushes have high yield strength. Since the silicate assemblage typical of IIE irons can be formed by melting only 15% of H-chondrite silicate, Taylor concluded that the IIE irons must not have formed in a core. Watson silicate, however, appears to have formed by complete melting of H-chondrite silicate, thus the Taylor argument does not apply here. Because the metal composition is typical of IIE irons (Wasson, pers. comm.), we conclude that the total melting of chondritic silicate was a local phenomenon.

A surface or near surface location may have been the reason the Watson H-chondrite mass became engulfed in metal in the first place. A IIE impactor onto an H-chondritic surface, or vice versa, could cause melting and incorporation of the two types of materials with each other. Such a site would permit the variety of cooling histories we have inferred for Watson, Kodaikanal, and Netschaëvo based on whether a mass was actually on the surface, if it lay under some overburden, or if it were originally buried and then suddenly erupted onto the surface. It was clearly a site susceptible to subsequent impact and the kind of shock event recorded in the metal. A surface or near-surface position would explain the break-off of the Watson meteoroid 8 Ma ago without shock profound enough to reset radiometric clocks.

Niemeyer (1980) favors two parent bodies as sources for the two age groups of IIE irons with silicates: the 3.8 Ga young group, Netschaëvo, Kodaikanal and (now) Watson; and the 4.5 Ga old group, Weekeroo Station, and Colomera. The case for a single source for the young group is strengthened by the metallographic and silicate similarities between Watson and Kodaikanal.

CONCLUSIONS

Watson provides a link between the stage of incorporation of H-chondrite material into metal (such as seen in Netschaëvo) and the evolution of highly fractionated globular silicate masses seen in many IIE irons. This study also confirms a direct link between the H-group chondrites and the IIE irons, a link which was established by their derivation from the same oxygen isotope reservoir (Clayton *et al.*, 1983). Thus, Watson fills an important gap in understanding the sequence of events that took place in the evolution of the IIE-H parent body or bodies. The ability to determine as much as we have about these events stems from the fortunate association of a large, unfractionated silicate mass within metal. Both of these regimes, silicate and metal, offer separate insights that must ultimately agree with each other.

Acknowledgments—We wish to thank Mr. Tim Rose for the preparation of the samples, Dr. John T. Wasson for making available his INAA data on Watson metal, Drs. G. F. Herzog and S. Xue for making available their ^{10}Be and ^{26}Al measurements, Dr. Julian R. Goldsmith and Mr. Munir Humayun for helpful discussions. This work was supported by grants from: the National Aeronautics and Space Administration, NAG 9-498 (E.O.), NAG 9-51 (R.N.C.), NAG 9-111 (A.M.D.), NAG 9-54 (L.G.), NAG 9-48 (M.E.L.) and NAG 9-47 (I.M.S.); the National Science Foundation, EAR 89-20584 (R.N.C); and the Department of Energy, DE-FG07-80ER1 072SJ(M.E.L.).

Editorial handling: J. Goldstein

REFERENCES

ARMSTRONG J., KENNEDY A., CARPENTER P. AND ALBEE A. (1990) Petrography and trace element chemistry of Colomera (IIE) silicate inclusions: Rhyolitic plums in the pudding (abstract). *Lunar Planet. Sci.* **20,** 22–23.

AXON H. J. (1968) The metallographic structure of the Kodaikanal meteorite. *Mineral. Mag.* **36,** 687–690.

BEGEMANN F. AND SCHULTZ L. (1988) The influence of bulk chemical composition on the production rate of cosmogenic nuclides in meteorites (abstract). *Lunar Planet. Sci.* **19,** 51–52.

BEGEMANN F., WEBER H. W. AND HINTENBERGER H. (1976) Rare gases and ^{36}Cl in stony-iron meteorites: Cosmogenic elemental production rates, exposure ages, diffusion losses and thermal histories. *Geochim. Cosmochim. Acta* **40,** 353–368.

BEGEMANN F. LI Z., SCHMITT-STRECKER S., WEBER H. W. AND XU Z. (1985) Noble gases and the history of the Jilin meteorite. *Earth Planet. Sci. Lett.* **72,** 247–262.

BENCE A. E. AND BURNETT D. S. (1969) Chemistry and mineralogy of the silicates and metal of the Kodaikanal meteorite. *Geochim. Cosmochim. Acta* **33,** 387–407.

BEVAN A. W. R., KINDER J. AND AXON H. J. (1979) A metallographic study of the iron meteorite Verkhne Dnieprovsk (B 51183). *Mineral. Mag.* **43,** 149–154.

BILD R. AND WASSON J. (1977) Netschaëvo: A new class of chondritic meteorite. *Science* **197,** 58–62.

BLAU P. J., AXON H. J. AND GOLDSTEIN J. I. (1973) Investigation of the Canyon Diablo metallic spheroids and their relationship to the breakup of the Canyon Diablo meteorite. *J. Geophys. Res.* **78,** 363–374.

BUCHWALD V. F. (1971) Tritium loss resulting from cosmic annealing. *Chemie der Erde* **30,** 33–57.

BUCHWALD V. F. (1975) *Handbook of Iron Meteorites.* Univ. of California Press, Berkeley, California.

BUCHWALD V. F. AND CLARKE R. S., JR. (1987) The Verkhne Dnieprovsk iron meteorite specimens in the Vienna collection and the confusion of Verkhne Dnieprovsk with Augustinovka. *Meteoritics* **22,** 121–135.

BUNCH T. E. AND OLSEN E. (1968) Potassium feldspar in Weekeroo Station, Kodaikanal, and Colomera iron meteorites. *Science* **160,** 1223–1225.

BUNCH T. E., KEIL K. AND OLSEN E. (1970) Mineralogy and petrology of silicate inclusions in iron meteorites. *Contrib. Mineral. Petrol.* **25,** 297–340.

BURNETT D. S. AND WASSERBURG G. J. (1967) Evidence for the formation of an iron meteorite at 3.8 x 10^9 years. *Earth Planet. Sci. Lett.* **2,** 137–147.

CLARKE R. S., JR. AND GOLDSTEIN J. I. (1978) Schreibersite growth and its influence on the metallography of coarse-structured iron meteorites. *Smithsonian Contrib. Earth Sci.* **21.** Smithsonian Press, Washington, D. C. 80 pp.

CLAYTON R. N., MAYEDA T. K., OLSEN E. AND PRINZ M. (1983) Oxygen isotope relationships in iron meteorites. *Earth Planet Sci. Lett.* **65,** 229–232.

CLAYTON R. N., MAYEDA T. K., GOSWAMI J. N. AND OLSEN E. J. (1991) Oxygen isotope studies of ordinary chondrites. *Geochim. Cosmochim. Acta* **55,** 2317–2337.

CROZAZ G., PELLAS P., BOUROT-DENISE M, DE CHAZAL S., FIÉNI C., LUNDBERG L. AND ZINNER E. (1989) Plutonium, uranium and rare earths in the phosphates of ordinary chondrites—The quest for a chronometer. *Earth Planet. Sci. Lett.* **93,** 157–169.

DAVIS A. M., MACPHERSON G. J., CLAYTON R. N., MAYEDA T. K., SYLVESTER P. J., GROSSMAN L., HINTON, R. W. AND LAUGHLIN J. R. (1991) Melt solidification and late-stage evaporation in the evolution of a FUN inclusions from the Vigarano C3V chondrite. *Geochim. Cosmochim. Acta* **55,** 621–637.

DODD R. T. *(1981) Meteorites: A Petrologic-Chemical Synthesis.* Cambridge Univ. Press, Cambridge, U. K. 368 pp.

EUGSTER O. (1988) Cosmic-ray production rates for ^{3}He, ^{21}Ne, ^{38}Ar, ^{83}Kr and ^{126}Xe in chondrites based on ^{81}Kr-Kr exposure ages. *Geochim. Cosmochim. Acta* **52,** 1649–1662.

EVENSEN N. M., HAMILTON P. J. AND O'NIONS R. K. (1978) Rare-earth abundances in chondritic meteorites. *Geochim. Cosmochim. Acta* **42,** 1199–1212.

FAHEY A. J., GOSWAMI J. N., MCKEEGAN K. D. AND ZINNER E. (1987) ^{26}Al, ^{244}Pu, ^{50}Ti, REE, and trace element abundances in hibonite grains from CM and CV meteorites. *Geochim. Cosmochim. Acta* **51,** 329–350.

HAMPEL W. AND SCHAEFFER O. A. (1979) ^{26}Al in iron meteorites and the constancy of cosmic ray intensity in the past. *Earth Planet. Sci. Lett.* **42,** 348–358.

HINTENBERGER H., SCHULTZ L., WÄNKE H. AND WEBER H. W. (1967) Helium- und Neonisotope in Eisenmeteoriten und der Tritium-verlust in Hexahedriten. *Z. Naturforsch.* **22a,** 780–787.

JAROSEWICH E. (1990) Chemical analyses of meteorites: A compilation of stony and iron analyses. *Meteoritics* **25,** 323–337.

LINDSLEY D. (1983) Pyroxene thermometry. *Amer. Mineral.* **68,** 477–493.

LINDSTROM M. M., CROZAZ G. AND ZINNER E. (1985) REE in phosphates from lunar highlands cumulates: an ion probe study (abstract). *Lunar Planet. Sci.* **16,** 493–494.

LINGNER D., HUSTON T. J., HUTSON M. AND LIPSCHUTZ M. E. (1987) Chemical studies of H chondrites–I. Mobile trace elements and gas retention ages. *Geochim. Cosmochim. Acta* **51,** 727–739.

LIPSCHUTZ M. E. (1992) Meteorites. In *Encyclopedia of the Solar System* (eds. P. Weissman and T. V. Johnson), submitted.

LIPSCHUTZ M. E., BISWAS S. AND MCSWEEN H. Y., JR. (1983) Chemical characteristics and origin of H chondrite regolith breccias. *Geochim. Cosmochim. Acta* **47,** 169–179.

MARTI K. (1967) Trapped xenon and the classification of chondrites. *Earth Planet. Sci. Lett.* **2,** 193–196.

MORGAN J. W. (1971). Uranium (92). In *Handbook of Elemental Abundances in Meteorites* (ed. B. Mason), pp. 529–548. Gordon and Breach, New York.

MORGAN J. W., JANSSENS M.-J., TAKAHASHI H., HERTOGEN J. AND ANDERS E. (1985) H-chondrites: Trace element clues to their origin. *Geochim. Cosmochim. Acta* **49,** 247–259.

NAKAMURA N. (1974) Determination of REE, Fe, Mg, Na and K in carbonaceous and ordinary chondrites. *Geochim. Cosmochim. Acta* **38,** 757–775.

NIEMEYER S. (1980) I-Xe and ^{40}Ar-^{39}Ar dating of silicate from Weekeroo Station and Netschaëvo IIE iron meteorites. *Geochim. Cosmochim. Acta* **44,** 33–44.

OLSEN E. AND BUNCH T. E. (1984) Equilibration temperatures of the ordinary chondrites: A new evaluation. *Geochim. Cosmochim. Acta* **48,** 1363–1365.

OLSEN E. AND JAROSEWICH E. (1971) Chondrules: First occurrence in an iron meteorite. *Science* **174,** 583–585.

OSADCHII EU. G., BARYSHNIKOVA G. V. AND NOVIKOV G. V. (1981) The Elga meteorite: Silicate inclusions and thermal metamorphism. *Proc. Lunar Planet. Sci. Conf.* **12th,** 1049–1068.

PARSONS I. (1978) Alkali-feldspars: Which solvus? *Phys. Chem. Minerals* **2,** 199–213.

PRINZ M., NEHRU C., DELANEY J., WEISBERG M. AND OLSEN E. (1983) Globular silicate inclusions in IIE irons and Sombrerete: Highly fractionated minimum melts (abstract). *Lunar Planet. Sci.* **14,** 616–617.

ROSS M, PAPIKE J. J. AND SHAW K. W. (1969) Exsolution textures in amphiboles as indicators of subsolidus thermal histories. *Mineral. Soc. Amer. Special Paper* **2,** 275–299.

RUBIN A. E., KEIL K., TAYLOR G. J., MA M.-S., SCHMITT R. A. AND BOGARD D. D. (1980) Derivation of a heterogeneous lithic fragment in the Bovedy L-group chondrite from impact-melted porphyritic chondrules. *Geochim. Cosmochim. Acta* **45,** 2213–2228.

SACK R. AND GHIORSO M. (1991) Chromian spinels as petrogenetic indicators: Thermodynamics and petrological applications. *Amer. Mineral.* **76,** 827–847.

SAIKUMAR V. AND GOLDSTEIN J. I. (1988) An evaluation of the methods to determine the cooling rates of iron meteorites. *Geochim. Cosmochim. Acta* **52,** 715–726.

SANZ H. G., BURNETT D. S. AND WASSERBURG G. J. (1970) A precise ^{87}Rb/^{87}Sr age and initial ^{87}Sr/^{86}Sr for the Colomera iron meteorite. *Geochim. Cosmochim. Acta* **34,** 1227–1239.

SCHULTZ L. (1967) Tritium loss in iron meteorites. *Earth Planet. Sci. Lett.* **2,** 87–89.

SCHULTZ L. (1990) Planetary noble gases in H3- and H4-chondrite falls (abstract). *Meteoritics* **25,** 405–406.

SCHULTZ L. AND KRUSE H. (1989) Helium, neon, and argon in meteorites–A data compilation. *Meteoritics* **24,** 155–172.

SCHULTZ L., WEBER H. W. AND BEGEMANN F. (1991) Noble gases in H-chondrites and potential differences between Antarctic and non-Antarctic meteorites. *Geochim. Cosmochim. Acta* **55,** 59–66.

SCOTT E. R. D. (1982) Origin of rapidly solidified metal-troilite grains in chondrites and iron meteorites. *Geochim. Cosmochim. Acta* **46,** 813–823.

SCOTT E. R. D. AND WASSON J. T. (1976). Chemical classification of iron meteorites– VIII. Groups IC, IIE, IIIF and 97 other irons. *Geochim. Cosmochim. Acta* **40,** 103–115.

SNYDER G. A., TAYLOR L. A., LIU Y.-G. AND SCHMITT R. A. (1992). Petrogenesis of the western highlands of the moon: Evidence from a diverse group of whitlockite-rich rocks from the Fra Mauro formation. *Proc. Lunar Planet. Sci. Conf.* **22nd,** 399–416.

SYLVESTER P. J., GROSSMAN L. AND MACPHERSON G. J. (1992) Refractory inclusions with unusual chemical compositions from the Vigarano carbonaceous chondrite. *Geochim. Cosmochim. Acta* **56,** 1342–1363.

TAYLOR G. J. (1991) Differentiation without core formation: S-Asteroids and stony-iron meteorites (abstract). *Lunar Planet.Sci.* **22,** 1385–1386.

VILCSEK E. AND WÄNKE H. (1963) Cosmic ray exposure ages and terrestrial ages of stone and iron meteorites derived from ^{36}Cl and ^{39}Ar measurements. *Radioactive Dating, I. A. E. A. Wien,* 381–393.

VOSHAGE H. (1962) Eisenmeteorite als Raumsonden für die Untersuchung des Intensitätsverlaufes der kosmischen Strahlung während der letzten Milliarden Jahre. *Z. Naturforsch.* **17a,** 422–432.

VOSHAGE H. (1982) Investigations of cosmic-ray-produced nuclides in iron meteorites. 4. Identification of noble gas abundance anomalies. *Earth Planet. Sci. Lett.* **61,** 32–40.

VOSHAGE H. (1984) Investigations of cosmic-ray-produced nuclides in iron meteorites. 6. The Signer-Nier model and the history of the cosmic radiation. *Earth Planet. Sci. Lett.* **71,** 181–194.

VOSHAGE H. AND FELDMAN H. (1979) Investigations on cosmic-ray-produced nuclides in iron meteorites. 3. Exposure ages, meteoroid sizes and sample depths determined by mass spectrometric analyses of potassium and rare gases. *Earth Planet Sci. Lett.* **45,** 293–308.

VOSHAGE H., FELDMAN H. AND BRAUN O. (1983) Investigations on cosmic-ray-produced nuclides in iron meteorites. 5. More data on the nuclides of potassium and noble gases, on exposure ages and meteoroid sizes. *Z. Naturforsch.* **38a,** 273–280.

WANG M.-S. AND LIPSCHUTZ M. E. (1990) Labile trace elements in lunar meteorite Yamato 86032. *Proc. NIPR Symp. Antarct. Meteorites* **3rd,** 19–26.

WASSON J. T. AND WANG J. (1986) A nonmagmatic origin of the group-IIE iron meteorites. *Geochim. Cosmochim. Acta* **50,** 725–732.

WOLF S. F. AND LIPSCHUTZ M. E. (1992) Multivariate statistical analysis of labile trace elements in H chondrites: Evidence for meteoroid streams (abstract). *Meteoritics* **27,** 308–309.

ZÄHRINGER J. (1966) Primordial argon and the metamorphism of chondrites. *Earth Planet. Sci. Lett.* **1,** 379–382.

ZINNER E. AND CROZAZ G. (1986) A method for the quantitative measurement of rare earth elements in the ion microprobe. *Int. Jour. Mass Spectrom. Ion Proc.* **69,** 17–38.